Journal of Theoretical Biology 459 (2018) 67–78

Contents lists available at ScienceDirect

Journal of Theoretical Biology

journal homepage: www.elsevier.com/locate/jtb

Optimal control to develop therapeutic strategies for metastatic castrate resistant prostate cancer

Jessica J. Cunningham[a,b,*], Joel S. Brown[a,c], Robert A. Gatenby[a,d], Kateřina Staňková[b,e]

[a] Department of Integrated Mathematical Oncology, Moffitt Cancer Center & Research Institute, Tampa, Florida, USA
[b] Department of Data Science and Knowledge Engineering, Maastricht University, Maastricht, The Netherlands
[c] Department of Biological Sciences, University of Illinois at Chicago, Chicago, Illinois, USA
[d] Department of Diagnostic Imaging and Interventional Radiology, Moffitt Cancer Center & Research Institute, Tampa, Florida, USA
[e] Delft Institute of Applied Mathematics, Delft University of Technology, Delft, The Netherlands

ARTICLE INFO

Article history:
Received 7 May 2018
Revised 13 September 2018
Accepted 19 September 2018
Available online 20 September 2018

Keywords:
Metastatic castrate-resistant prostate cancer
Optimal control
Evolutionary game theory
Competitive release
Eco-evolutionary dynamics
Adaptive therapy

ABSTRACT

In metastatic castrate resistant prostate cancer (mCRPC), abiraterone is conventionally administered continuously at maximal tolerated dose until treatment failure. The majority of patients initially respond well to abiraterone but the cancer cells evolve resistance and the cancer progresses within a median time of 16 months. Incorporating techniques that attempt to delay or prevent the growth of the resistant cancer cell phenotype responsible for disease progression have only recently entered the clinical setting. Here we use evolutionary game theory to model the evolutionary dynamics of patients with mCRPC subject to abiraterone therapy. In evaluating therapy options, we adopt an optimal control theory approach and seek the best treatment schedule using nonlinear constrained optimization. We compare patient outcomes from standard clinical treatments to those with other treatment objectives, such as maintaining a constant total tumor volume or minimizing the fraction of resistant cancer cells within the tumor. Our model predicts that continuous high doses of abiraterone as well as other therapies aimed at curing the patient result in accelerated competitive release of the resistant phenotype and rapid subsequent tumor progression. We find that long term control is achievable using optimized therapy through the restrained and judicious application of abiraterone, maintaining its effectiveness while providing acceptable patient quality of life. Implementing this strategy will require overcoming psychological and emotional barriers in patients and physicians as well as acquisition of a new class of clinical data designed to accurately estimate intratumoral eco-evolutionary dynamics during therapy.

1. Introduction

Like most late stage cancers, metastatic prostate cancer is usually incurable. Even when initial therapies successfully decrease the tumor burden, the patient will eventually succumb to the disease. Standard cancer therapy conventionally applies drugs at maximum tolerable dose (MTD) based on the implicit assumption that maximizing cancer cell death will result in the best outcome. While this “treat to kill” strategy is intuitively appealing, it may be evolutionarily unwise because it leads to strong selection for resistant cell phenotypes by eliminating potentially competing sensitive cell phenotypes. This concept, termed “competitive release”, where one of two species competing for the same resource disappears thereby allowing the remaining competitor to utilize the resource more fully than it could in the presence of the first species, is well-described in other evolutionary settings such as ecology and pest-management (Connell, 1961; Zeilinger et al., 2016).

Evolutionary approaches used in these other fields, particularly pest management, accept that complete eradication of an undesired species is not always possible. Similarly, in common disseminated cancers (such as prostate, lung, breast, colorectal, pancreatic etc.), decades of clinical observations have clearly demonstrated that a cure, with currently used therapies, is not possible. For these cancers the goal of cancer treatment should shift to its long term control, essentially turning cancer into a chronic disease (Enriquez-Navas et al., 2016). Adaptive therapy is one method implementing this treatment philosophy explicitly integrating principles from ecology and evolution by actively modulating therapy during treatment. Treatment is applied to control the cancer cell population sensitive to drug and judiciously removed to let the remaining sensitive cell population suppress the proliferation of the resistant cell population.

* Corresponding author.
E-mail address: jessica.cunningham@maastrichtuniversity.nl (J.J. Cunningham).

https://doi.org/10.1016/j.jtbi.2018.09.022
0022-5193/

Here we will focus on treatment of metastatic prostate cancer (mPC). The majority of mPC cancer cells at the time of initial diagnosis require systemic testosterone for survival and proliferation. We designate these cells T^+. Upon diagnosis, androgen deprivation therapy (ADT) is used as a means of chemical castration providing an initially effective means of reducing the tumor burden of these T^+ cells. However, under continued ADT, the tumor begins to grow again within 1 to 3 years as the tumor cells evolve resistance. This leads to metastatic castrate resistant prostate cancer (mCRPC). Two resistant cell phenotypes are typically found in mCRPC tumors. Some cells evolve mutations in the androgen receptor (AR) itself and downstream variations in AR signaling that allow proliferation completely independent of testosterone. We designate these androgen-independent cells as T^-. Alternatively, some cells upregulate *CYP*17α which allows the cancer cells to synthesize testosterone through a cholesterol pathway involving an auto-stimulatory loop. These testosterone producing cells (designated T^P) can secrete enough testosterone to bring intra-tumoral levels of testosterone within functional pre-ADT levels (Mohler et al., 2004; Montgomery et al., 2008). As a result, the locally supplied testosterone from T^P cells can support the proliferation of T^+ cells despite continued ADT.

Abiraterone, an inhibitor of *CYP*17α, was developed to provide a therapy for mCRPC by inhibiting the residual production of testosterone in the adrenal cortex as well as the T^P cells production of testosterone. As ADT treatment is continued during abiraterone therapy, the further reduction of testosterone by abiraterone suppresses both the T^P and T^+ cells. Continuous therapy with abiraterone as standard of care often provides a sharp reduction in tumor burden and a period of remission by presumably eliminating both the T^+ and T^P tumor cell populations. With a median time of 16 - 17 months, abiraterone therapy fails, tumor burdens increase, and patients again experience tumor growth. The elimination of the T^+ and T^P cells releases the T^- cells from competition for space and resources allowing them to proliferate freely. No targeted therapies exist for these T^- cells and cytotoxic chemotherapies become the only late stage option until further disease progression and eventual patient death.

An adaptive therapy in mCRPC would aim to delay or completely prevent the competitive release of the T^- cells while maintaining an acceptably low tumor burden. In support of the feasibility of such a goal, a recent preliminary trial significantly prolonged the time to progression of mCRPC by giving abiraterone until the prostate specific antigen, known as PSA (surrogate for tumor burden), dropped to below 50% of its starting level, and then removing therapy until PSA returned to the pre-treatment level. The adaptive treatment schedule was supported by a game-theoretic model of mCRPC that considered the eco-evolutionary dynamics and interactions of the three cell types discussed above (Zhang et al., 2017). Both the clinical trial and the mathematical model showed that evolution-based therapies can significantly prolong time to progression while reducing cumulative dose when compared to current standard of care. The initial success in theory and in practice invites an exploration of more sophisticated time-dependent applications of abiraterone. It is likely that there are significant opportunities to further improve the outcomes with sufficient understanding of the underlying dynamics of cancer cells.

Here we start with the model of Zhang et al. (2017) and frame it as an optimal control problem. Optimal control for time-dependent problems involves recognizing dynamic state variables (for our model these will be the population sizes and frequencies of the T^+, T^P and T^- cells), an objective (i.e. tumor size) and a control that can be varied in time (treatment dose schedule). Optimization techniques can isolate values of the control which minimizes the objective over some fixed or varied time horizon of the model. The majority of past optimal control models of cancer therapy define the objective as minimizing total tumor volume following the standard goal of "treat to cure". Swan and Vincent (1977) and Swan (1980, 1988) provide the first applications of optimal control theory to treating cancer. Optimal control theory has since been used to investigate cytotoxic chemotherapies, cell cycle chemotherapies, radiotherapy, and immunotherapies (Ainseba and Benosman, 2010; Benzekry and Hahnfeldt, 2013; Cappuccio et al., 2007; Castiglione and Piccoli, 2006; 2007; Coldman and Murray, 2000; Ghaffari and Naserifar, 2010; Kim et al., 2014; Ledzewicz et al., 2012; Ledzewicz and Schaettler, 2016; Ledzewicz and Schattler, 2004; 2005; 2008; Murray, 1990a; 1990b; Nanda et al., 2007; Swierniak and Smieja, 2005; Villasana et al., 2010; Zhu et al., 2015). There are also optimal control studies in prostate cancer focusing on the optimal schedule of ADT (Hirata and Aihara, 2015; Hirata et al., 2018). Engelhart (2011) and others have emphasized the importance of selecting the objective more carefully (Carrere, 2017; Engelhart et al., 2011; Hadjiandreou and Mitsis, 2014). Since we know that the "treat to cure" objective may be unfeasible, in this paper we specifically explore alternative objectives with the goal of long-term tumor control.

First, we model continuous abiraterone therapy based on the clinical standard of care using maximum tolerable dose. Second, from the Zhang clinical trial, we know that the adaptive therapy was effective with as little as 20% of maximal dose. With this in mind, we determine the optimal control therapy by minimizing total tumor density using only 20% of the cumulative total abiraterone dose. Third, we consider the optimal dose schedule when the therapy objective is to minimize the variance of tumor burden over some time horizon. Gatenby (2009) showed the effectiveness of this objective in maintaining long term tumor control in an in-vivo experiment using carboplatin on OVCAR xenographs in mice (Gatenby et al., 2009). Lastly, we consider the objective of directly controlling the T^- cell population by preventing competitive release. Under this control algorithm, the goal is to minimize the population density of the T^- cells over the course of therapy. Finally, we discuss the clinical implications of these different optimal control treatments and the patient information needed for clinically implementing and evaluating our model′s predictions.

2. Tumor growth model

We extend the model from Zhang et al. (2017) and consider mCRPC as an evolutionary game. Evolutionary game models of cancer can include both the ecological and evolutionary consequences of therapy and they can suggest evolutionarily enlightened therapies (Altrock et al., 2015; Basanta and Anderson, 2018; Basanta et al., 2012; Bayer et al., 2018; Brown, 2016; Gatenby, 2009; Gatenby et al., 2009; Gatenby and Vincent, 2003; Gupta et al., 2015; Kam et al., 2014; Silva et al., 2012; Tomlinson, 1997). For mCRPC, the evolutionary game is played among cancer cells possessing different strategies that influence the production of and need for testosterone. We consider three types of cancer cells as players in mCRPC:

- T^+ cells requiring exogenous androgen;
- T^P cells expressing 17α-hydroxy/17,20-lyase (CYP17α) and producing testosterone; and
- T^- cells that are androgen-independent.

2.1. Initial Lotka–Volterra model

We use a model inspired by Lotka–Volterra (LV) competition equations to describe the interactions between T^+, T^P and T^- cell types, $i \in \mathcal{T} = \{T^+, T^P, T^-\}$. The LV equations require parameterization of growth rates, r_i, carrying capacities, K_i, and competition coefficients, α_{ij}, comprising a 3×3 competition matrix $A = \left(\alpha_{ij}\right)$. We

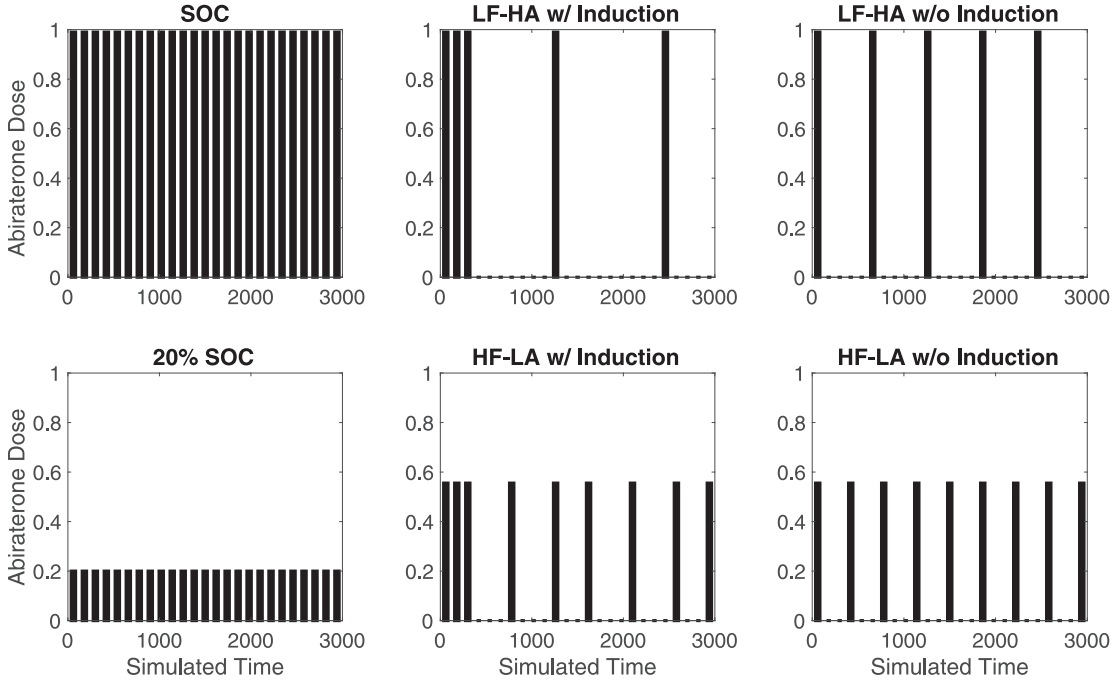

Fig. 1. Non-Optimized Treatment Schedules. Panel (a) shows standard of care with the maximum tolerable dose applied at each subinterval, with a cumulative dose of 25. Panel (b) shows 20% dose with a cumulative dose of 5. The remaining four panels (c)–(f) show the metronomic therapies, each with the cumulative dose of 5: (c) low frequency - high amplitude metronomic therapy with induction, (d) high frequency - low amplitude metronomic therapy with induction, (e) low frequency - high amplitude metronomic therapy without induction, and (f) high frequency - low amplitude metronomic therapy without induction.

can describe the instantaneous rate of change in the population size of cancer cell types $i \in \mathcal{T}$, $\dot{y}_i = \frac{dy_i}{dt}$ as

$$\dot{y}_i = r_i y_i \left(1 - \frac{\sum_{j \in \mathcal{T}} \alpha_{ij} y_j}{K_i} \right). \tag{1}$$

2.2. Parameter estimation

2.2.1. Growth rates

We derived the growth rates of the three subpopulations in (1) from the measured doubling times of representative cell lines. The LNCaP cell line (ATCC@CRL-1740) is representative of T^+ cells as they are androgen dependent. LNCaP cells have a measured doubling time of 60 hours. The T^P growth rate is based off the H295R cell line (ATCC@CRL-2128), with a doubling time of 48 hours. Finally, we base the T^- growth rate is based on the PC-3 cell line, with a doubling time of 25 hours. From these doubling times the growth rates of the T^+, T^P, and T^- cells would be 0.27726, 0.34657, and 0.66542, respectively. These cell line derived growth rates (units of per day) are unlikely to be biologically feasible within a tumor environment with limited resources. We therefore scale these growth rates to $r_{T^+} = 2.7726 \cdot 10^{-3}$, $r_{T^P} = 3.4657 \cdot 10^{-3}$, and $r_{T^-} = 6.6542 \cdot 10^{-3}$ for our model. Scaling the growth rates does not affect the steady states/evolutionarily stable states of the underlying evolutionary game, as r_i in (1) is scalable.

2.3. Carrying capacities without abiraterone treatment

The carrying capacity of the T^+ cell population derives entirely from utilizing the endogenous testosterone produced by the T^P cells as the majority of the exogenous testosterone provided by the body has been removed by continuous ADT. Therefore, we assume that the carrying capacity of T^+ is a linear function of the density of T^P cells as defined by $K_{T^+} = \mu \cdot y_{T^P}$. While the exact value of T^+ cells that can be symbiotically supported by the androgens created by T^P cells is unknown, its value above one accounts for the fact that the T^P cells incur the cost of producing the androgens while the T^+ cells require no resources to obtain the needed androgens. In this way, we set the symbiosis coefficient μ to $\mu = 1.5$.

As in Zhang et al. (2017) we set the carrying capacities of T^P and T^- cells in the absence of abiraterone to $K_{T^P} = K_{T^-} = 10000$.

2.4. Carrying capacities with abiraterone treatment

Therapies can be modeled in Lotka-Volterra models of tumor growth in multiple ways. For example, a chemotherapy will alter the growth rates r_i, hormonal or targeted therapies will alter carrying capacities K_i, and cytotoxic therapies will introduce an additional mortality term. Experimental evidence shows that abiraterone does not act as a chemotherapy nor a cytotoxic therapy in prostate cancer cell lines (Grossebrummel et al., 2016). In this way, consistent with Zhang et al. (2017), abiraterone therapy reduces the ability of T^+ and T^P cells to acquire an essential resource, testosterone, and is modeled as a direct reduction in the carrying capacity of T^P and indirectly that of T^+.

The abiraterone dose during a control region $\Lambda(t) \in [0, 1]$ equals to 0 if no drug is given at time t and equals to 1 if the maximum tolerable dose is applied. Abiraterone affects the cells in two ways. Firstly, abiraterone treatment diminishes the T^P cells ability to fully utilize the CYP17α pathway to convert cholesterol into androgens. Therefore, in our model the carrying capacity of T^P is significantly decreased to $K_{T^P} = 100$ when abiraterone is administered at full dose. To allow for intermediate doses of abiraterone, we assume the following relationship between K_{T^P} and dose:

$$K_{T^P}(t) = -9900\Lambda(t) + 10000 \tag{2}$$

Secondly, because abiraterone inhibits the production of testosterone from T^P cells, the T^+ cells that are symbiotically supported by the androgens created by T^P cells are affected. In this way, the symbiosis coefficient μ is lowered linearly to a minimum value of 0.5 as abiraterone dose increases to the maximum tolerable

Table 1
Coefficients for fitness matrix *A*.

coefficient values						
α_{12}	α_{13}	α_{21}	α_{23}	α_{31}	α_{32}	Group
0.7	0.8	0.4	0.5	0.6	0.9	Best responder
0.7	0.8	0.4	0.6	0.5	0.9	Responder
0.7	0.9	0.4	0.6	0.5	0.8	Non responder

Table 2
Initial population densities.

Initial population densities			
$y_{T^+}(0)$	$y_{T^P}(0)$	$y_{T^-}(0)$	Group
606.06	757.58	$1.94 \cdot 10^{-10}$	Best Responder
560.36	747.59	47.10	Responder
319.63	707.76	273.97	Non Responder

dose:

$$\mu(t) = -\Lambda(t) + 1.5. \tag{3}$$

2.5. Competition coefficients

The matrix of competition coefficients defines the interactions between the three cell types and characterizes the payoff interactions within the evolutionary game. The values of α_{ij} are qualitative approximations where each competition coefficient describes the effect of type j cells on the growth rate of type i cells. The intra-cell type coefficients are set to $\alpha_{ii} = 1$. The relative values of the remaining coefficients are derived from literature and professional judgment of prostate oncologists. T^+ cells with no exogenous testosterone are in general the least competitive cell type, and the competitive effect of T^- cells is stronger on T^P cells than on T^+ cells. These two principles lead to the following series of inequalities: $\alpha_{31} > \alpha_{21}$, $\alpha_{32} > \alpha_{12}$, $\alpha_{13} > \alpha_{23}$, $\alpha_{13} > \alpha_{12}$, $\alpha_{23} > \alpha_{21}$, and $\alpha_{32} > \alpha_{31}$. As in both Zhang et al. (2017) and You et al. (2017) we assume the inter-cell type coefficients have values from the set {0.4, 0.5, 0.6, 0.7, 0.8, 0.9}. Using these values, there are 22 biologically plausible matrices that satisfy the above inequalities. Based on the frequencies of T^- at the equilibrium, we can divide these 22 simulated patients into one of three categories: best responders, responders, and non-responders. Here we choose one matrix from each category to analyze in detail as shown in Table 1.

2.6. Linear stability analysis of the model with $K_{T^P} \in [0, 10000]$

While the population dynamics of our evolutionary game between cancer cells defined by (1) superficially resembles Lotka–Volterra competition equations, the symbiotic relationship between the T^P and T^+ cells significantly changes the structure of the system. If one only considers tumors with T^P and T^- cells or T^+ and T^P cells then the dynamics and their stability properties match the 2-species Lotka-Volterra competition equations. When considering a tumor with just T^+ and T^P cells, the T^P cells experience competition from the T^+ cells in accord with the matrix of competition coefficients. However, the net interaction effect of T^P on T^+ is the difference between the symbiosis and competition coefficients. Since the symbiosis coefficient μ has been set to 1.5, and the competition coefficients are always less than one, the net effect of T^P on T^+ is positive. Furthermore, $\frac{\dot{y}_{T^+}}{y_{T^+}}$ is the interaction coefficient that gives the effect of changing the population size of T^P on the population growth rate of T^+. In the standard Lotka-Volterra equations these interaction coefficients are negative and independent of population sizes. In our model, all of the interaction coefficients but the one describing the effects of T^P on T^+ are negative and independent of the cancer cells population sizes. The effect of y_{T^P} on $\frac{dy_{T^+}}{dt}$ is positive (reflecting the public good provided by T^P to T^+) and the magnitude of this effect declines with y_{T^P}. Moreover, in the standard Lotka-Volterra equations, carrying capacities are constant and independent of species populations sizes. The positive and density-dependent interaction coefficients of T^P on T^+ significantly change the underlying dynamics and stability of the system from that of standard Lotka-Volterra models.

To illustrate this, we performed the linear stability analysis for all three representative matrices with respect to the value of $K_{T^P} \in [0, 10000]$. In all three cases, for K_{T^P} between 0 and a certain threshold the stable steady point which coincides with the attractor of the dynamics of our extended Lotka–Volterra model contains only T^- cells. Increasing K_{T^P} results in a stable steady point which includes both T^P and T^- cells. Increasing K_{T^P} further results in the stable steady point including all three types of cells. Interestingly, for the best responder case only, relatively close to the carrying capacity of T^P cells a steady point exists where only T^+ and T^P cells are present. This stability analysis illustrates how abiraterone treatment (which reduces the T^P carrying capacity) can push the system defined by (1) towards competitive release of T^-. A full stability analysis is included in S2.

3. Implementation

All simulations were performed in Matlab as follows: The system of differential equations in (1) was discretized using the 4th order Runge-Kutta method. The maximum time of simulation was set to $t_f = 3000$ [days] with 6000 discretization steps. The time horizon [0, 3000] was divided into 25 subintervals each with 120 simulated days (240 discretized steps). This simulates the time between patient clinical visits where changes to treatment can be made. Within each interval between clinical visits, abiraterone dose is held constant. Within a subinterval, the dose of abiraterone could take on a value of $\Lambda \in [0, 1]$. Abiraterone naive tumor growth where no abiraterone is given is modeled where $\Lambda = 0$ for all subintervals. This naive tumor growth is used to set the initial population densities for each representative patient shown in Table 2 (See S1 for detailed explanation). The growth rates and carrying capacities are set to values discussed in Section 2.2.

Six predetermined treatment schedules that are typically used in the clinic are analyzed to compare against novel optimized treatment schedules (see Fig. 1). First, clinical standard of care maximum tolerable dose is modeled where $\Lambda = 1$ for all subintervals resulting in a cumulative dose of 25. We constrain all remaining predetermined treatment schedules and optimized treatment schedules to have a cumulative dose of 5 (20% maximum tolerable dose). This allows comparisons between treatment schedules to be based on changes in distribution of a predetermined cumulative dose instead of changes of the dose itself.

Second, we modeled a constant 20% of maximum dose ($\Lambda = 0.2$ for all subintervals.) The value of Λ affects carrying capacities within the subinterval as described in Eqs. (2) and (3). When $\Lambda(t) = 0.2$, the carrying capacity of K_{T^P} equals 8020 and the symbiotic coefficient equals $\mu = 1.3$.

The four remaining predetermined schedules are metronomic and included combinations of high amplitude/low frequency versus low amplitude/high frequency dosing and no induction period versus a 3 subinterval induction period (see Fig. 1). These metronomic treatment schedules also adhere to the constraint of cumulative dose equal to 5 allowing direct comparison with the other simulated therapies based on 20% of standard of care.

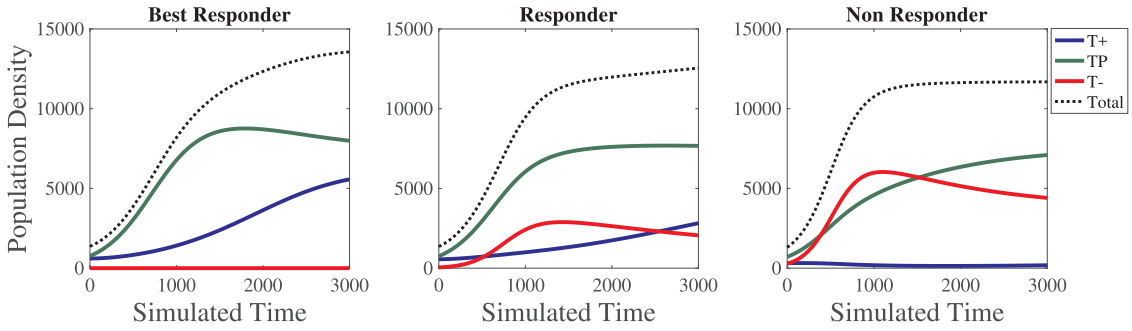

Fig. 2. Cell population dynamics under no abiraterone treatment. In all three cases, the total tumor burden reaches levels where we would expect patient discomfort and eventual death. The T^- cell population for the best responder patient is initially minimal and does not increase due to competition from T^P and T^+ cells. For the responder and non responder patients the frequency of T^- cells initially increases but is then decreased due to the inter-cell type competition. These dynamics provide a baseline to compare the effects of various Abiraterone treatment schedules.

4. Optimal control problem

We formulate a control problem to seek the best distribution of a cumulative abiraterone dose of 5 to achieve a specific therapy objective. In this way, the optimization algorithm iterates over varying distributions of $\Lambda \in [0, 1]$ across the 25 subintervals. To find the time-dependent optimal dose distribution we used the Matlab nonlinear constrained optimization toolbox (`fmincon`), where 100 optimization replicates were performed for each of the three patient cases and each objective. For all optimization replicates the treatment schedule is initialized with a random dosing schedule with a total cumulative dose of 5. The nonlinear optimization algorithm keeps this constraint active, while allowing each $\Lambda(t)$ to vary between 0 and 1.

The goal is to find $\Lambda(\cdot) = (\Lambda(t))_{t\in[0,t_f]}$ that according to the following three possible objectives for patient care:

- Minimizing average tumor volume:

$$\min_{\Lambda(\cdot)} \frac{1}{t_f} \int_0^{t_f} \sum_{i\in\mathcal{T}} y_i(t)\, \mathrm{d}t$$

- Minimizing tumor mass variance:

$$\min_{\Lambda(\cdot)} \frac{1}{t_f} \int_0^{t_f} \left(\sum_{i\in\mathcal{T}} y_i(t) - \overline{\sum_{i\in\mathcal{T}} y_i(t)} \right)^2 \mathrm{d}t$$

- Minimizing average T^- density:

$$\min_{\Lambda(\cdot)} \frac{1}{t_f} \int_0^{t_f} y_{T^-}(t)\, \mathrm{d}t$$

5. Results

5.1. No treatment

Fig. 2 shows the population dynamics of each cell type for each of the three patient categories (interaction matrices) under no abiraterone. The total tumor burden grows to levels where we would expect patient discomfort and eventual death. The best responder tumor becomes dominated by T^+ and T^P cells as the T^- population declines towards extinction. The responder patient has a mix of all three cell subtypes. The non-responder patient shows a tumor with only T^P and T^- cells present.

5.2. Standard of care

For the best responder patient (Fig. 3), this treatment led to an apparent cure. During the simulation the density of the tumor cells appeared negligible. There was however a non-zero cumulative density of T^- cells at the end of the simulation ($\approx$21.86). This is approximately $2 \cdot 10^4$ times larger than when no abiraterone is given ($\approx 1.12 \cdot 10^{-4}$). If abiraterone was continued indefinitely, relapse would occur as the T^- cells would eventually grow to their carrying capacity. This relapse caused by T^- cells occurs more quickly in the majority of patients as seen with both the responder and non-responder patients. The responder patient (Fig. 4) had a slightly longer response time than the non-responder patient (Fig. 5) due to the lower initial density of T^- cells at the initiation of therapy. In all cases of the model, continuous abiraterone therapy resulted in a tumor comprised entirely of T^- cells. In this way, following the initial success of therapy, the rate of treatment failure would be determined primarily by the population size of T^- at the onset of therapy (see Table 2).

5.3. Standard of care: 20% constant treatment

20% constant treatment dosing was surprisingly ineffective for the best responder patient showing strikingly similar results to no treatment at all (Fig. S1). The best responder resulted in a tumor composed entirely of T^+ and T^P cells with an overall burden that was about 20% less than no therapy. In both the responder and non-responder patients, the T^- cell type became the dominant subtype.

5.4. Metronomic low frequency - high amplitude - with induction

Under this metronomic schedule the best responder patient maintained a tumor burden comprised mainly of T^P cells that increased and decreased in number during the on and off cycling of abiraterone. This remaining population continually suppressed the T^- population, providing a long-term control not possible with maximum tolerable dose. In the responder and non-responder patient the induction period eliminated the T^+ and T^P populations and caused the competitive release of T^-. Consequently, the subsequent drug holidays and doses of abiraterone were ineffective. In this way, the disease trajectory became nearly equivalent to the full dose standard of care treatment schedule.

5.5. Metronomic low frequency - high amplitude - without induction

Removing the induction period for the best responder again maintained a tumor burden comprised mainly of T^P cells that continually suppressed the T^- population. For the responder and non-responder patients the first two high amplitude doses of abiraterone were enough to eliminate the T^+ and T^P cells and the disease trajectory became nearly equivalent to the full dose standard of care treatment schedule.

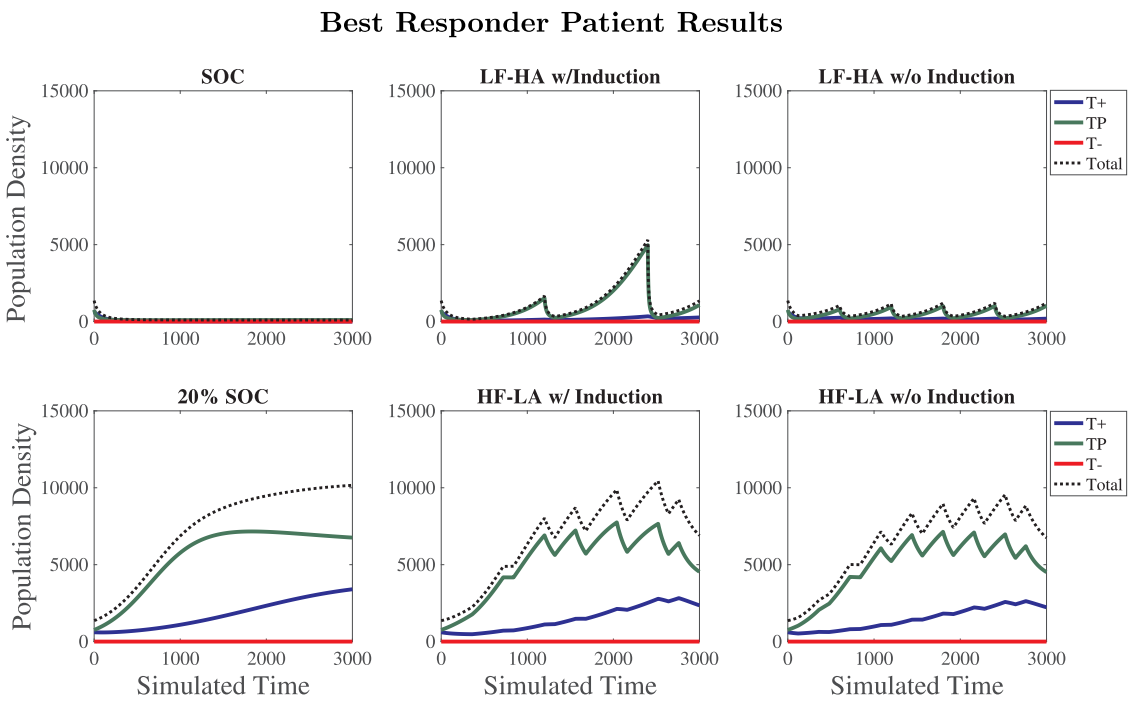

Fig. 3. Population dynamics of best responder patient for non optimized treatment schedules. Panels (a)–(f) depict population dynamics for treatments (a)–(f) from Fig. 1, respectively. SOC results in an apparent cure while 20% SOC is relatively ineffective. All metronomic therapies provide tumor control with varying underlying tumor dynamics.

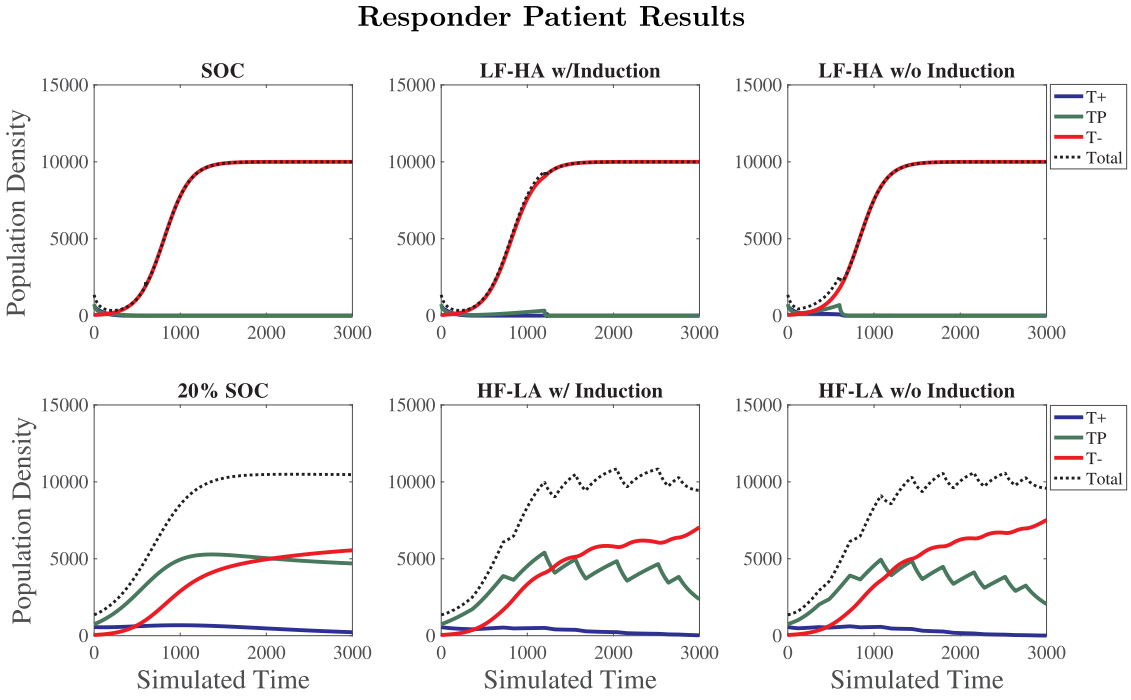

Fig. 4. Population dynamics of responder patient for non optimized treatment schedules. Panels (a)–(f) depict population dynamics for treatments (a)–(f) from Fig. 1, respectively. SOC of care and metronomic therapies with induction periods result in early competitive release of the T^- population. 20% SOC and the metronomic therapies without an induction period delay this T^- competitive release by preserving a population of T^P cells.

5.6. Metronomic high frequency - low amplitude - with induction

This metronomic schedule administered treatment twice as often but at half the dose of the high amplitude simulations. For the best responder patient, these lower doses allowed a greater density of T^+ and T^P cells to remain in the population. While this maintained a higher overall tumor burden, the tumor burden is controlled. For the responder and non responder patients, the lower doses maintained a mix of T^P and T^- cells and the competitive release of the T^- population was delayed.

5.7. Metronomic high frequency - low amplitude - without induction

The elimination of the induction period with the high frequency low dose metronomic therapy does not demonstrably change the

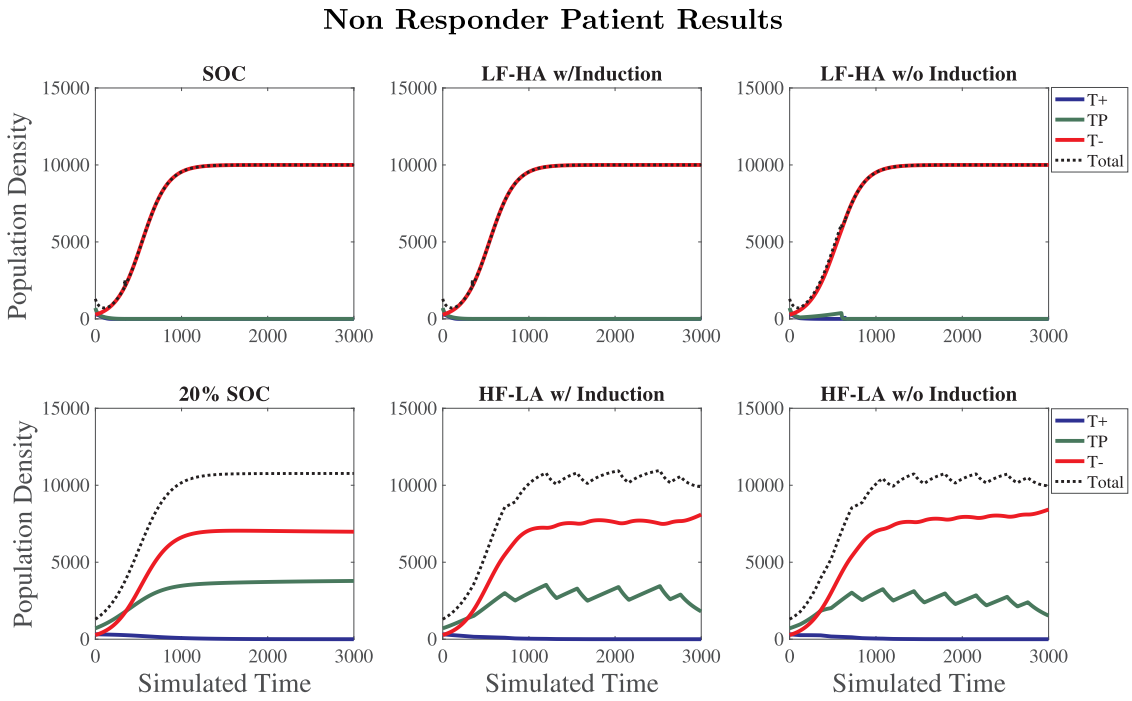

Fig. 5. Population dynamics of non responder patient for non optimized treatment schedules. Panels (a)–(f) depict population dynamics for treatments (a)–(f) from Fig. 1, respectively. Similar to the responder patient, SOC of care and metronomic therapies with induction periods result in early competitive release of the T^- population. The larger initial density of T^- cells in this non responder patient leads to an accelerated T^- competitive release compared to the responder patient in the 20% SOC and the metronomic therapies without an induction period.

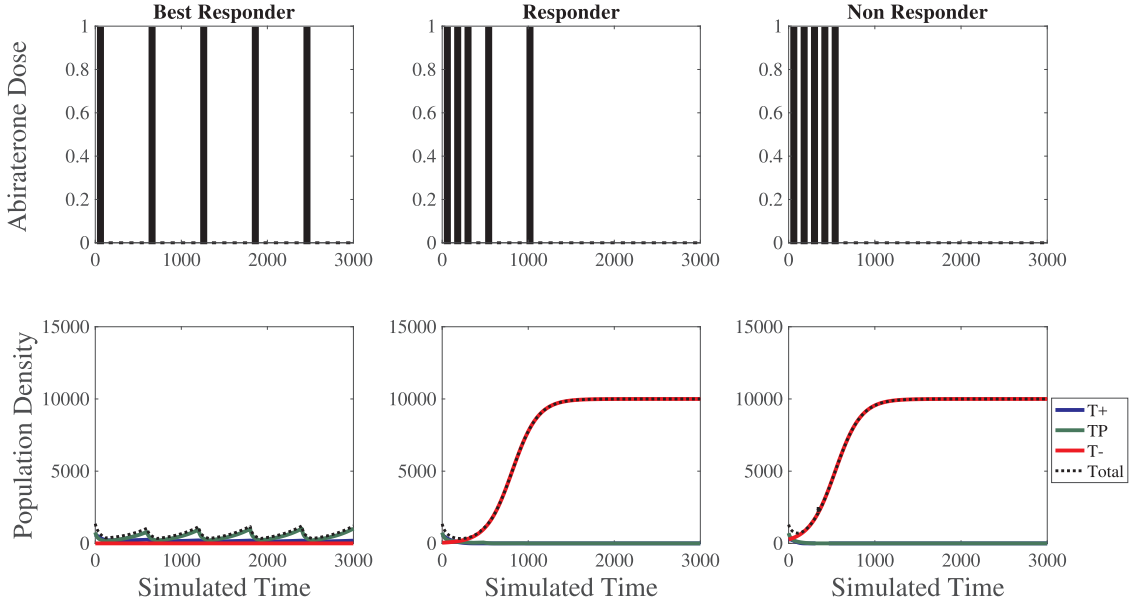

Fig. 6. Optimized results for minimizing total tumor volume on three representative patients. For the best responder patient, the optimized schedule maintains a very small total tumor burden comprised mainly of T^p cells. Administering abiraterone early in the responder and non responder patients completely eliminate the T^+ and T^p cell types, leaving only the T^- cell type to contribute to the total tumor volume.

trajectory of the disease for any of the three patient types compared to with the induction period.

Optimization case studies

We sought the best therapy based on optimal control for the three different objectives of minimizing total tumor volume (Fig. 6), variance in tumor size (Fig. 7), and the cumulative density of T^- cells (Fig. 8). For all of these cases, the cumulative abiraterone dose was constrained to 5.

For some of the 100 replicate simulations, the optimal control algorithm found different local minima. Except when minimizing the total tumor variance, the treatment schedules associated with the local minima involved an on-off bang-bang style controller where $\Lambda(t)$ equals either 1 or 0. Because of this, we subsequently analyzed all possible bang-bang treatment schedules of abiraterone to find the corresponding minimal objective values. In the following section the bang-bang results are shown. When the objective is minimizing variance in tumor size for responder and non respon-

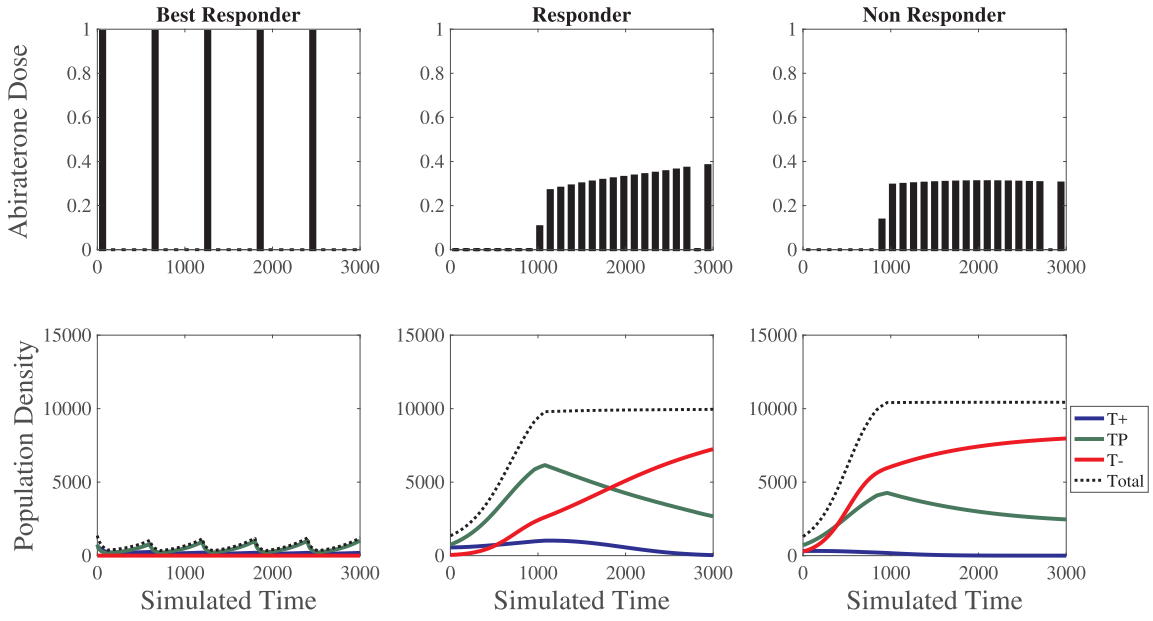

Fig. 7. Optimized results for minimizing tumor volume variance on three representative patients. The responder patient shows that minimizing the total tumor volume and minimizing the variance require the same treatment schedule (compare to Fig. 6). For the responder and non responder patients, once treatment is initiated, the total tumor volume is kept constant, resulting in a low tumor variance. While the tumor is a constant size, the underlying composition is changing from a T^p dominated tumor to a T^- dominated tumor.

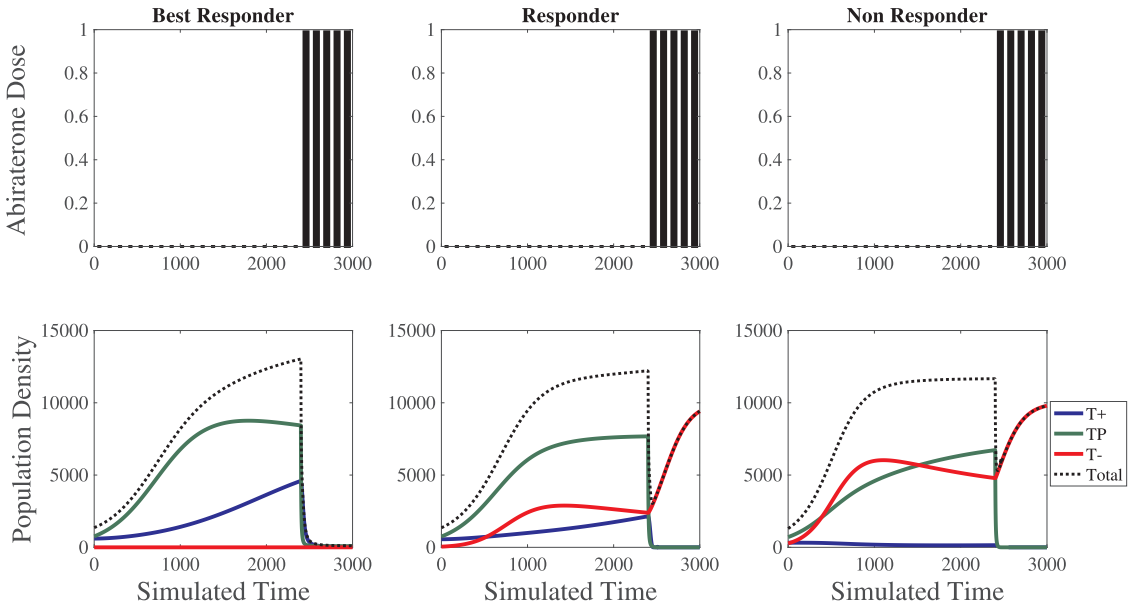

Fig. 8. Optimized results for minimizing T^- density on three representative patients. All three patient types result in the same optimized treatment schedule showing all five doses of abiraterone in the last five subintervals. The T^- cell density is kept low due to inter-cell type competition. Only when the doses of abiraterone are given do the T^- cells grow uncontrolled.

der patients, the optimal schedule from the minimization solver is shown (Fig. 7).

5.8. Optimized treatment schedules for minimizing cumulative tumor volume

By trying to minimize the cumulative population sizes of the three cell types, the physician is either attempting a “treat to cure” or to maintain a minimum average tumor burden over the time horizon (Fig. 6). In all three cases the optimal treatment was bang-bang. For the best responder patient, the optimized schedule was the high amplitude - low frequency metronomic therapy without induction. This was a fascinating result in that giving bursts of high dose abiraterone is more effective at minimizing total tumor volume over time than giving a constant 20% dose. The total tumor burden was only 8.7% that of the 20% consistent standard of care. For the responder and non-responder patients the optimized abiraterone treatment schedule was to give abiraterone early and completely eliminate the T^+ and T^p cell types, leaving only one cell type to contribute to the total tumor volume. In this way, the total tumor volume in both the responder and non responder patients can only be lowered to the total tumor volume reached by full 100% standard of care, 4.40×10^7 and 4.92×10^7, respectively.

5.9. Minimizing tumor variance

Fig. 7 shows the optimal control therapy for minimizing the variance of tumor burden over the time of simulation. The optimized treatment schedule for minimizing variance in the best responder patient was the same as minimizing cumulative tumor volume (Fig. 6), as minimizing the volume minimizes the variance. For the responder and non responder cases, the optimal controller resulted in intermediate levels of dosing. Since there is no target for overall tumor burden, the treatment schedule delayed giving any treatment until the tumor had grown from the initial tumor size to approximately 10,000. Then, low doses were given to maintain a constant tumor volume for the remainder of the time horizon. The objective resulted in a constant tumor volume, even as competitive release of the T^- cells occurred during treatment, similar to the high frequency low dose metronomic therapy.

5.10. Minimizing total T- density

The sequence of doses in Fig. 8 minimized the cumulative population size of T^- over the time horizon. All three patient types receive bang-bang treatment, delaying administration of abiraterone for as long as possible. All the doses were back loaded to the end of the time horizon. By not treating the T^+ and T^p populations with abiraterone for as long as possible, those populations were able to suppress the growth of the T^- population, thus minimizing the objective value. In all cases, only giving no abiraterone at all resulted in a lower cumulative density of T^-.

Time to competitive release and comparing objective functions

We create a quantitative measure of the time to competitive release of T^- as the time at which T^- becomes the majority of the tumor composition as described below. Frequency of T^- at time $t \in [0, t_f]$ is calculated as

$$p(t) = \frac{y_{T^-}(t)}{\sum_{i \in \mathcal{T}} y_i(t)}$$

The frequency of the T^+ and T^p together at time t can be calculated as

$$q(t) = \frac{y_{T^+}(t) + y_{T^p}(t)}{\sum_{i \in \mathcal{T}} y_i(t)}$$

The time of competitive release t_{CR} is defined as the first moment of time t when

$$p(t) > q(t),$$

i.e.

$$t_{CR} \stackrel{\text{def}}{=} \min\{t \in [0, T] : p(t) > q(t)\}.$$

Table 3 shows this time of competitive release for each treatment schedule in our case studies.

For the best responder patient the density of T^- cells is very low for all cases, which accounts for the absence of competitive release during the time horizon. Attempting to cure the patient by giving standard of care or optimizing the treatment schedule to minimize total tumor density results in the largest density of T^- cells and the earliest time to competitive release for the responder and non-responder patients. The minimization of the T^- population results in the latest time to competitive release and lowest total density of T^- of any treatment schedules (excluding giving no treatment at all).

In Tables S1, S2, and S3 we quantitatively compare the objective function values of all ten treatment schedules for the “Best Responder”, “Responder”, and “Non-responder” patients, respectively.

Table 3
Time to competitive release for all patients.

Treatment schedule	Best responder	Responder	Non responder
No Treatment	> 3000	> 3000	458
SOC	> 3000	203	60
20% SOC	> 3000	2388	410
LFHA w/Induction	> 3000	203	60
LFHA wo/Induction	> 3000	366	60
HFLA w/Induction	> 3000	1319	624
HFLA wo/Induction	> 3000	1461	391
Volume	> 3000	203	60
Variance	> 3000	1950	458
T-	> 3000	2416	2402

Robustness to jitter of bang-bang treatment schedules

Seven of the nine optimal control treatment schedules were bang-bang. This means that at all decision points, either the minimum or maximum amount of abiraterone was applied. For these cases, we performed a full analysis of all possible combinations of bang-bang control. This allows confirmation that the optimization algorithm was finding the true minimum of all possible bang-bang treatment schedules and to study the robustness to jitter (shifting the administration of treatment to adjacent control points) of the optimized bang-bang control. This is clinically relevant, as it addresses the robustness of an optimal control therapy. How exact does the optimal control algorithm need to be to reap the benefits of a dynamic controller? If small deviations in treatment schedule result in large changes in patient outcome, it may prove difficult to successfully implement these schedules. On the other hand, if small deviations in treatment schedule do not drastically affect long term patient outcomes, then clinical application may be achievable without compromising patient health.

The bang-bang control of minimizing the cumulative total tumor volume is quite robust to jitter of the treatment schedule for all three patient types. The bang-bang control of minimizing tumor variance for the best responder patient is also quite robust. As the optimized treatment schedules for the responder and non-responder patient were not approaching a bang-bang control, they are not included in this analysis. The bang-bang control of minimizing the cumulative T^- population for the best responder patient is also robust. This is due to the fact that there is very little T^- population in these tumors and changing the treatment schedule does not affect the value of this objective within the time of the simulation. Of most interest is the fact that bang-bang control of minimizing the cumulative T^- population in the responder and non-responder patient is **not** robust to jitter. Giving the first dose in the back-loaded treatment schedule just one subinterval earlier in the simulation time significantly increases the total T^- density. This shows the importance of delaying the administration of abiraterone for as long as possible if the objective is to minimize the resistant T^- population.

A full expansion of the robustness of bang-bang treatment schedules can be seen in section S4.

6. Discussion

Using an evolutionary game theoretic model of metastatic castrate resistant prostate cancer we studied the effects on the underlying tumor composition from standard of care, metronomic, and newly proposed optimized treatment schedules of the drug abiraterone acetate. Under the assumption that metastatic disease can not be completely eliminated, instead we studied the success of these therapies in terms of management of the disease with the ultimate goal to delay or completely prevent the competitive re-

lease of the T^- cells while maintaining an acceptably low tumor burden.

High dose density standard of care, high dose density metronomics, and front-loaded dosing schedules such as metronomic therapies with induction periods all empirically and in our model provide a dramatic initial response in minimizing tumor burden. Our model shows that this dramatic initial response is caused by the elimination of abiraterone sensitive cancer cells (T^P). These effects, in all cases, are inevitably short lived as the elimination of the sensitive cancer cells allows unconstrained growth of the resistant T^- cells. Our model also shows that induction periods used in metronomic schedules cause this competitive release explaining why clinical trials in metronomic therapies are only non-inferior, not superior, to full dose standard of care treatment (Bouche et al., 2014; Mehta et al., 2009; Montagna et al., 2014). These types of treatments fail to result in a cure and are ill-designed to manage cancer as a chronic disease, as the time that abiraterone is effective is short lived.

In contrast, the optimized schedule for minimizing tumor variance and the low dose metronomic schedules successfully delay the competitive release of resistant T^- populations. By reducing dose density, the models show that the sensitive populations are eliminated at a slower pace, not resulting in a dramatic decrease in tumor burden but instead resulting in a longer-term tumor maintenance. These reduced dose density schedules can greatly increase the time that abiraterone is effective and better manage cancer as a chronic disease.

The null case of never administering abiraterone is the only schedule that completely prevents the competitive release of the resistant T^- population. As this is obviously not an acceptable treatment option, our results show that the closest we can get to completely preventing competitive release is to back-load any abiraterone doses as late as possible in the treatment time. Interestingly, requiring the administration of 20% maximum tolerable dose proved to be a high enough dose density to cause competitive release late in treatment. Though by delaying, the patient directly gains progression free survival and lengthens the time that abiraterone is effective.

Combining the lessons learned from these three treatment schedule types, the overarching conclusion is two fold: 1) delay giving any treatment for as long as possible, and 2) when treatment is required, give the smallest dose possible. In a true clinical scenario, the timing and dose of abiraterone will need to be determined on an individual patient basis. Each patient will have their unique tolerable level of tumor burden that will most likely be defined using a combination of blood marker indicators and quality of life measures. Only when the patient is approaching their personal limit of tumor burden should any abiraterone be given. The abiraterone dose given at this time should be the **minimum** dose required to provide the patient acceptable measures of blood markers and quality of life.

To successfully implement this type of low dose density delayed therapy correctly for each individual patient, proper measurements of the underlying tumor composition and quality of life will be required. While there are many quality of life measures available (Resnick and Penson, 2012), the measure of underlying tumor composition proves much more difficult. The importance of measuring the underlying tumor composition is becoming apparent in other hormonal cancers such as breast cancer (Yi et al., 2014), yet equivalent measures in mCRPC are difficult as biopsies of disseminated bone disease in mCRPC patients is both expensive and painful. The new technology of androgen receptor immunohistochemistry "liquid biopsy" from routine blood draws or the development of a high affinity androgen receptor ligand for imaging like that of PSMA PET could potentially provide the required information, though these techniques are currently far from clinically feasible (Krishnamurthy et al., 2017; Maurer et al., 2016; Meo et al., 2017; Yee et al., 2016).

Certainly, future refinements of the base mathematical model and optimization techniques will improve predictions (Staňková et al., 2018). For example, the true nature of the symbiosis between the T^+ and T^P cells should be experimentally established using representative cell lines providing support for the parameterization of the competition coefficients and growth rates. Additionally, future analysis of PSA dynamics and patient data of disease progression in the ongoing clinical trial will provide quantitative parameter refinement that will greatly improve model predictions (Gause, 1934; Gregorio et al., 2016; Hardin, 1960; Orlando et al., 2013; Zhang et al., 2017). Analytical optimization techniques such as dynamic programming combined with generalized characteristics of the underlying Hamilton-Jacobi-Bellman equation could provide another way to solve the current model (Bellman, 1957; Melikyan, 1994; 1998). If this proves to be unfeasible, advanced heuristic methods, such as evolutionary computation, neural networks, and genetic and memetic studies, could be adopted in the optimal control scheme (Liang et al., 2006; Lobato et al., 2016; Tan et al., 2002; Tse et al., 2007).

Of most interest, if more sophisticated real-time patient specific measurements of mCRPC tumors become available, is to implement real-time model predictive control methods where the model and the corresponding optimal treatment schedule can be updated with each measure of the patient state during the treatment (Algoul et al., 2011; Moradi et al., 2013; Muros et al., 2017). A very important aspect of the real-time predictive model would be the ability to categorize each patient as quickly as possible in order to provide an optimal therapy prediction as early as possible. Fortunately, the results shown here predict the optimal treatment to delay competitive release of resistant subpopulations is invariably a low dose delayed therapy for all patient types. If this holds true, the time to optimize for each patient would be minimal.

While these extensions can provide more specific predictions, the results shown here provide a foundation of treatment scheduling options for management of cancer as a long term disease and the basic principles of the consequences of these treatment schedules on the underlying tumor dynamics.

7. Conclusion

With an increase in understanding of cancer as an evolutionary process, it is not unreasonable to propose a paradigm shift away from curing patients and towards a long term management strategy. In mCRPC, and potentially other cancers where resistance to therapy is the known cause of treatment failure, our study suggests that only when a patient is approaching their personal limit of tumor burden should treatment be initiated, and then only the **minimum** dose required to provide the patient acceptable measures of blood markers and quality of life should be administered. Understandably, advances in mathematical modeling, experimental techniques, and patient monitoring technology will be required to facilitate the psychological leap required for patients to implement this type of treatment schedules and potentially comfortably live with cancer as a long term manageable disease.

Acknowledgments

This work was supported by the European Union's Horizon 2020 research and innovation program (Marie Sklodowska-Curie grant agreement No 690817), the James S. McDonnell Foundation grant, Cancer therapy: Perturbing a complex adaptive system, a V Foundation grant, NIH/National Cancer Institute (NCI) R01CA170595, Application of Evolutionary Principles to Maintain

Cancer Control (PQ21), and NIH/NCI U54CA143970-05 [Physical Science Oncology Network (PSON)] Cancer as a complex adaptive system. The authors would like to thank Ralf Peeters for providing insight and expertise that greatly improved this research.

Supplementary material

Supplementary material associated with this article can be found, in the online version, at 10.1016/j.jtbi.2018.09.022.

References

Ainseba, B., Benosman, C., 2010. Optimal control for resistance and suboptimal response in CML. Math. Biosci. 227 (2), 81–93.

Algoul, S., Alam, M.S., Hossain, M.A., Majumder, M.A., 2011. Multi-objective optimal chemotherapy control model for cancer treatment. Med. Biol. Eng. Comput. 49, 51–65.

Altrock, P.M., Liu, L.L., Michor, F., 2015. The mathematics of cancer: integrating quantitative models. Nat. Rev. Cancer 12, 730–745.

Basanta, D., Anderson, A.R.A., 2018. Homeostasis back and forth: an ecoevolutionary perspective of cancer. Cold Spring Harb. Perspect Med. 7 (9). doi:10.1101/cshperspect.a028332.

Basanta, D., Scott, J.G., Fishman, M.N., Ayala, G., Hayward, S.W., Anderson, A.R.A., 2012. Investigating prostate cancer tumour stroma interactions: clinical and biological insights from an evolutionary game. Br. J. Cancer 106 (1), 174–181. doi:10.1038/bjc.2011.517.

Bayer, P., Brown, J.S., Staňková, K., 2018. A two-phenotype model of immune evasion by cancer cells. J. Theor. Biol. 455, 191–204. doi:10.1016/j.jtbi.2018.07.014. http://www.sciencedirect.com/science/article/pii/S0022519318303382.

Bellman, R., 1957. Dynamic Programming. Princeton University Press, Princeton, New Jersey.

Benzekry, S., Hahnfeldt, P., 2013. Maximum tolerated dose versus metronomic scheduling in the treatment of metastatic cancers. J. Theor. Biol. 335, 235–244.

Bouche, G., Andr, N., Banavali, S., Berthold, F., Berruti, A., Bocci, G., Brandi, G., Cavallaro, U., Cinieri, S., Colleoni, M., Curigliano, G., Desidero, T.D., Eniu, A., Fazio, N., Kerbel, R., Hutchinson, L., Ledzewicz, U., Munzone, E., Pasquier, E., Scharovsky, O.G., Shaked, Y., Strba, J., Villalba, M., Bertolini, F., 2014. Lessons from the fourth metronomic and anti-angiogenic therapy meeting, 24,25 june 2014, milan. Ecancermedicalscience 8, 463.

Brown, J.S., 2016. Why Darwin would have loved evolutionary game theory. Proc. R. Soc. B 283 (1838). Paper nr. 20160847.

Cappuccio, A., Castiglione, F., Piccoli, B., 2007. Determination of the optimal therapeutic protocols in cancer immunotherapy. Math. Biosci. 209 (1), 1–13.

Carrère, C., 2017. Optimization of an in vitro chemotherapy to avoid resistant tumours. J. Theor. Biol. 413, 24–33.

Castiglione, F., Piccoli, B., 2006. Optimal control in a model of dendritic cell transfection cancer immunotherapy. Bull. Math. Biol. 68 (2), 255–274.

Castiglione, F., Piccoli, B., 2007. Cancer immunotherapy, mathematical modeling and optimal control. J. Theor. Biol. 247 (4), 723–732.

Coldman, A.J., Murray, J.M., 2000. Optimal control for a stochastic model of cancer chemotherapy. Math. Biosci. 168 (2), 187–200.

Connell, J., 1961. The influence of interspecific competition and other factors on the distribution of the barnacle Chthamalus stellatus. Ecology 42 (4), 710–723.

Engelhart, M., Lebiedz, D., Sager, S., 2011. Optimal control for selected cancer chemotherapy ODE models: a view on the potential of optimal schedules and choice of objective function. Math. Biosci. 229 (1), 123–134.

Enriquez-Navas, P.M., Kam, Y., Das, T., Hassan, S., Silva, A., Foroutan, P., Ruiz, E., Martinez, G., Minton, S., Gillies, R.J., Gatenby, R.A., 2016. Exploiting evolutionary principles to prolong tumor control in preclinical models of breast cancer. Sci. Transl. Med. 8 (327), 327ra24.

Gatenby, R.A., 2009. A change of strategy in the war on cancer. Nature 459, 508–509.

Gatenby, R.A., Silva, A.S., Gillies, R.J., Frieden, B.R., 2009. Adaptive therapy. Cancer Res. 69 (11), 4894–4903.

Gatenby, R.A., Vincent, T.L., 2003. An evolutionary model of carcinogenesis. Cancer Res. 63, 6212–6220.

Gause, G.F., 1934. The Struggle For Existence (1st ed.). Williams and Wilkins..

Ghaffari, A., Naserifar, N., 2010. Optimal therapeutic protocols in cancer immunotherapy. Comput. Biol. Med. 40 (3), 261–270.

Gregorio, A.D., Bowling, S., Rodriguez, T.A., 2016. Cell competition and its role in the regulation of cell fitness from development to cancer. Dev. Cell 38, 621–634.

Grossebrummel, H., Peter, T., Mandelkow, R., Weiss, M., Muzzio, D., Zimmermann, U., Walther, R., Jensen, F., Knabbe, C., Zygmunt, M., Burchardt, M., Stope, M.B., 2016. Cytochrome p450 17a1 inhibitor abiraterone attenuates cellular growth of prostate cancer cells independently from androgen receptor signaling by modulation of oncogenic and apoptotic pathways. Int. J. Oncol. 48(2), 793–800.

Gupta, S., Gallaher, J., Lynch, C., Cook, L., Araujo, A., Scott, J., Dhillon, J., Pow-Sang, J., Basanta, D., 2015. Optimizing personalized treatment sequences in metastatic castration resistant prostate cancer using tumor-biomarker based computational modeling. J. Clin. Oncol. 33 (15_suppl). e16014–e16014. doi: 10.1200/jco.2015.33.15_suppl.e16014.

Hadjiandreou, M.M., Mitsis, G.D., 2014. Mathematical modeling of tumor growth, drug-resistance, toxicity, and optimal therapy design. IEEE Trans. Biomed. Eng. 61 (2), 415–425.

Hardin, G., 1960. The competitive exclusion principle. Science 131, 1292–1297.

Hirata, Y., Aihara, K., 2015. Ability of intermittent androgen suppression to selectively create a non-trivial periodic orbit for a type of prostate cancer patients. J. Theor. Biol. 384, 147–152.

Hirata, Y., Morino, K., Akakura, K., Higano, C.S., Aihara, K., 2018. Personalizing androgen suppression for prostate cancer using mathematical modeling. Sci. Rep. 8. Article number: 2673

Kam, Y., Das, T., Minton, S., Gatenby, R.A., 2014. Evolutionary strategy for systemic therapy of metastatic breast cancer: balancing response with suppression of resistance. Womens Health 10, 423–430.

Kim, K.S., Cho, G., Jung, I.H., 2014. Optimal treatment strategy for a tumor model under immune suppression. Comput. Math. Methods Med. 204. Paper nr. 206287.

Krishnamurthy, N., Spencer, E., Torkamani, A., Nicholson, L., 2017. Liquid biopsies for cancer: coming to a patient near you. J. Clin. Med. 6(1), 3.

Ledzewicz, U., Naghnaeian, M., Schättler, H., 2012. Optimal response to chemotherapy for a mathematical model of tumor-immune dynamics. J Math Biol 64 (3), 557–577.

Ledzewicz, U., Schaettler, H., 2016. Optimizing chemotherapeutic anti-cancer treatment and the tumor microenvironment: an analysis of mathematical models. Adv. Exp. Med. Biol. 936, 209–223.

Ledzewicz, U., Schättler, H., 2004. Controlling a model for bone marrow dynamics in cancer chemotherapy. Math. Biosci. Eng. 1 (1), 95–110.

Ledzewicz, U., Schättler, H., 2005. The influence of PK/PD on the structure of optimal controls in cancer chemotherapy models. Math. Biosci. Eng. 2 (3), 561–578.

Ledzewicz, U., Schättler, H., 2008. Optimal and suboptimal protocols for a class of mathematical models of tumor anti-angiogenesis. J. Theor. Biol. 252 (2), 295–312.

Liang, Y., Leung, K.S., Mok, T.S., 2006. A novel evolutionary drug scheduling model in cancer chemotherapy. IEEE Trans. Inf. Technol. Biomed. 10 (2), 237–245.

Lobato, F.S., Machado, V.S., Steffen Jr., V., 2016. Determination of an optimal control strategy for drug administration in tumor treatment using multi-objective optimization differential evolution. Comput. Methods Prog. Biomed. 131, 51–61.

Maurer, T., Eiber, M., Schwaiger, M., Gschwend, J.E., 2016. Current use of PSMA-PET in prostate cancer management. Nat. Rev. Urol. 13, 226–235.

Mehta, R.S., Jackson, D., Schubbert, T., 2009. Metronomic schedule of paclitaxel is effective in hormone receptor positive and hormone receptor negative breast cancer. J.f Clin. Oncol. 27, 3067–3068.

Melikyan, A.A., 1994. Necessary optimality conditions for a singular surface in the form of synthesis. J. Optim. Theory Appl. 82 (2), 203–217.

Melikyan, A.A., 1998. Generalized Characteristics of First Order PDEs: Applications in Optimal Control and Differential Games. Birkhäuser, Boston.

Meo, A.D., Bartlett, J., Cheng, Y., Pasic, M.D., Yousef, G.M., 2017. Liquid biopsy: a step forward towards precision medicine in urologic malignancies. Mol. Cancer 16, 80.

Mohler, J.L., Gregory, C.W., Ford III, O.H., Kim, D., Weaver, C.M., Petrusz, P., Wilson, E.M., French, F.S., 2004. The androgen axis in recurrent prostate cancer. Clin. Cancer Res. 10, 440–448.

Montagna, E., Cancello, G., Dellapasqua, S., Munzone, E., Colleoni, M., 2014. Metronomic therapy and breast cancer: a systematic review. Cancer Treatment Rev. 40, 942–950.

Montgomery, R.B., Mostaghel, E.A., Vessella, R., Hess, D.L., Kalhorn, T.F., Higano, C.S., True, L.D., Nelson, P.S., 2008. Maintenance of intratumoral androgens in metastatic prostate cancer: a mechanism for castration-resistant tumor growth. Cancer Res. 68, 4447–4454.

Moradi, H., Vossoughi, G., Salarieh, H., 2013. Optimal robust control of drug delivery in cancer chemotherapy: a comparison between three control approaches. Comput. Methods Prog. Biomed. 112 (1), 69–83.

Muros, F.J., Maestre, J.M., You, L., Staňková, K., 2017. Model predictive control for optimal treatment in a spatial cancer game. In: 2017 IEEE 56th Annual Conference on Decision and Control (CDC), pp. 5539–5544.

Murray, J.M., 1990. Optimal control for a cancer chemotherapy problem with general growth and loss functions. Math. Biosci. 98 (2), 273–287.

Murray, J.M., 1990. Some optimal control problems in cancer chemotherapy with a toxicity limit. Math. Biosci. 100 (1), 49–67.

Nanda, S., Moore, H., Lenhart, S., 2007. Optimal control of treatment in a mathematical model of chronic myelogenous leukemia. Math Biosci 210 (1), 143–156.

Orlando, P.A., Gatenby, R.A., Brown, J.S., 2013. Tumor evolution in space: the effects of competition colonization tradeoffs on tumor invasion dynamics. Front. Oncol. 3, 45.

Resnick, M.J., Penson, D.F., 2012. Quality of life with advanced metastatic prostate cancer. Urol. Clin. North Am. 39 (4), 505–515. doi:10.1016/j.ucl.2012.07.007.

Silva, A.S., Kam, Y., Khin, Z.P., Minton, S.E., Gillies, R.J., Gatenby, R.A., 2012. Evolutionary approaches to prolong progression-free survival in breast cancer. Cancer Res. 72, 6362–6370.

Staňková, K., Brown, J.S., Dalton, W.S., Gatenby, R.A., 2018. Optimizing cancer treatment using game theory: a review. JAMA Oncol. doi:10.1001/jamaoncol.2018.3395.

Swan, G.W., 1980. Optimal control in some cancer chemotherapy problems. Int. J. Syst. Sci. 11, 223–227.

Swan, G.W., 1988. General applications of optimal control theory in cancer chemotherapy. IMA J. Math. Appl. Med. Biol. 5 (5), 303–316.

Swan, G.W., Vincent, T.L., 1977. Optimal control analysis in the chemotherapy of IgG multiple myeloma. Bull. Math. Biol. 39 (3), 317–337.

Swierniak, A., Smieja, J., 2005. Analysis and optimization of drug resistant and phase-specific cancer chemotherapy models. Mathematical Biosciences and Engineering 2 (3), 657–670.

Tan, K.C., Khor, E.F., Cai, J., Heng, C.M., Lee, T.H., 2002. Automating the drug scheduling of cancer chemotherapy via evolutionary computation. Artif. Intell. Med. 25 (2), 169–185.
Tomlinson, I.P., 1997. Game-theory models of interactions between tumour cells. Eur. J. Cancer 33, 1495–1500.
Tse, S.M., Liang, Y., Leung, K.S., Lee, K.H., Mok, T.S., 2007. A memetic algorithm for multiple-drug cancer chemotherapy schedule optimization. IEEE Trans. Syst. Man Cybern. Part B 37 (1), 84–91.
Villasana, M., Ochoa, G., Aguilar, S., 2010. Modeling and optimization of combined cytostatic and cytotoxic cancer chemotherapy. Artif. Intell. Med. 50 (3), 163–173.
Yee, S.S., Lieberman, D.B., Blanchard, T., et al., 2016. A novel approach for next generation sequencing of circulating tumor cells. Mol. Genetics Genomic Med. 4(4), 395–406.
Yi, M., Huo, L., Koenig, K.B., Mittendorf, E.A., Meric-Bernstam, F., Kuerer, H.M., Bedrosian, I., Buzdar, U.A., Symmans, W.F., Crow, J.R., Bender, M., Shah, R.R., Hortobagyi, G.N., Hunt, K.K., 2014. Which threshold for ER positivity? a retrospective study based on 9639 patients. Ann. Oncol. 25(5), 1004–1011.
You, L., Brown, J.S., Thuijsman, F., Cunningham, J.J., Gatenby, R.A., Zhang, J., Staňková, K., 2017. Spatial vs. non-spatial eco-evolutionary dynamics in a tumor growth model. J. Theor. Biol. 435, 78–97.
Zeilinger, A.R., Olson, D.M., Andow, D.A., 2016. Competitive release and outbreaks of non-target pests associated with transgenic bt cotton. Ecol. Appl. 26, 1047–1054.
Zhang, J., Cunningham, J.J., Brown, J.S., Gatenby, R.A., 2017. Integrating evolutionary dynamics into treatment of metastatic castrate-resistant prostate cancer. Nat. Commun. 8 (1), 1816.
Zhu, J., Liu, R., Jiang, Z., Wang, P., Yao, Y., Shen, Z., 2015. Optimization of drug regimen in chemotherapy based on semi-mechanistic model for myelosuppression. J. Biomed. Inform. 57, 20–27.